

## DESIGN AND DEVELOPMENT OF BUNCH SHAPE MONITOR FOR FRIB MSU

S. Gavrilov<sup>†</sup>, A. Feschenko, Institute for Nuclear Research of Russian Academy of Sciences, Troitsk, Moscow, Russia

### Abstract

Bunch Shape Monitor was developed and tested in INR RAS for the Facility for rare isotope beams to fulfil the requirements of a half a degree phase resolution for 80.5 MHz FRIB operating frequency. The configuration of the  $\lambda/4$ -type RF-deflector based on the parallel wire lines with the shorting jumper and capacitive plates was selected. Special separation of secondary electrons by energy is foreseen to decrease a possible influence of the electrons detached from the ions in the wire target. Peculiarities of the design and development process are described. Results of laboratory tests are presented.

### INTRODUCTION

The operation principle of the Bunch Shape Monitor (BSM), developed in INR RAS, is based on the technique of a coherent transformation of a temporal bunch structure into a spatial charge distribution of low energy secondary electrons through a transverse RF-scanning [1, 2] and is clear from Fig. 1.

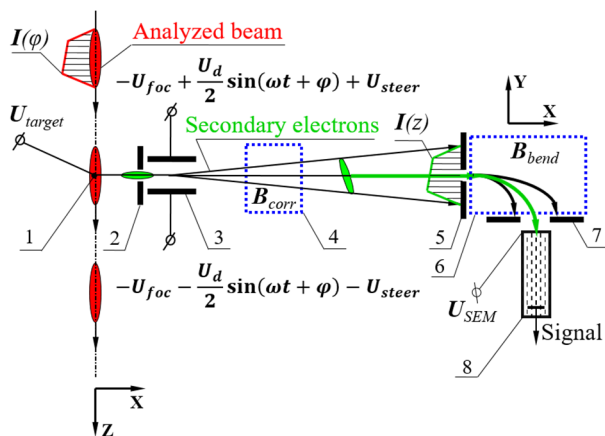


Figure 1: BSM scheme: 1 – tungsten wire target, 2 – inlet collimator, 3 – RF-deflector combined with electrostatic lens, 4 – correcting magnet, 5 – outlet collimator, 6 – bending magnet, 7 – registration collimator, 8 – secondary electron multiplier.

The series of the analysed beam bunches crosses the wire target 1 which is at a high negative potential about -10 kV. Interaction of the beam with the target results in emission of low energy secondary electrons, which characteristics of importance for bunch shape measurements are practically independent of beam energy and charge states of ions, so the monitor can be used for any location along the accelerator without design modification (Fig. 2).

<sup>†</sup> s.gavrilov@gmail.com

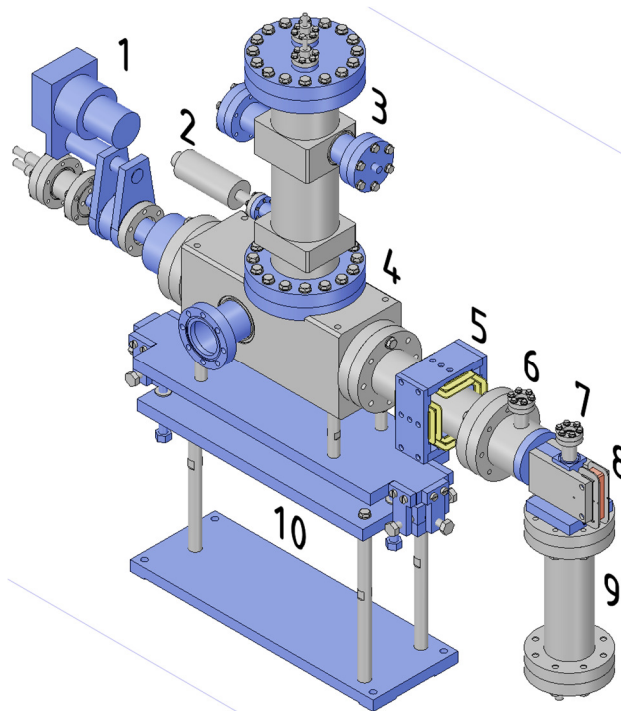


Figure 2: BSM design: 1 – target actuator, 2 – tuner, 3 – RF-deflector, 4 – BSM box, 5 – quadrupole + dipole correcting magnet, 6, 7 – viewports for optical control of e-beam, 8 – bending magnet, 9 – SEM-detector, 10 – support with 3D-adjustment.

The electrons are accelerated by electrostatic field and move almost radially away from the target. A fraction of the electrons passes through inlet collimator 2 and enters RF-deflector 3, where electric field is a superposition of electrostatic focusing and steering fields and RF-deflecting field with a frequency equal to the second harmonic of RF-field frequency in the linac: 161 MHz.

Passed electrons are scanned by the RF-field and an intensity of electrons passed through outlet collimator 5 represents a fixed point of the longitudinal phase distribution of the primary beam. Another points can be obtained by changing the phase of the deflecting field with respect to the RF-reference. If the phase of the deflecting field is adjusted in a wide range, then the bunch can be observed twice per the period of the deflecting field.

By adjusting the steering voltage one can change the measured phase position of the observed bunches and obtain the periodicity of bunches to be exactly equal to  $\pi$ . If the bunch duration is larger than  $\pi$ , the intensities corresponding the phase points differed by  $\pi$  are superimposes and the results of bunch shape measurements become wrong.

### RF-DEFLECTOR

BSM deflector is a RF-cavity with electrical length  $\lambda/4$ , based on parallel wire lines with capacitive plates (Fig. 3).

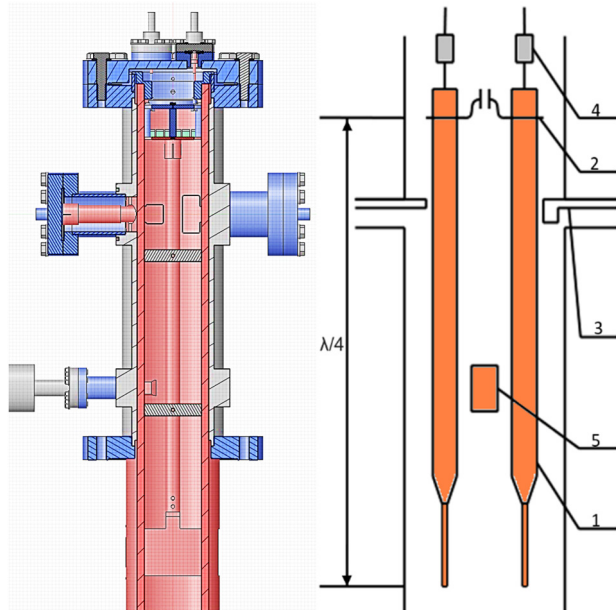


Figure 3: Cut plane and schematic diagram of  $\lambda/4$ -type RF-deflector of FRIB BSM.

Two electrodes 1 with deflecting plates are supported by ceramic insulators. The resonant frequency is adjusted by moving a short 2. The short consists of two collets connected by ceramic capacitors. Coupling loops 3 are used to drive the cavity and to detect the RF-signal. Focusing potentials are supplied through ceramic 1 M $\Omega$  resistors 4 which are used to diminish the influence of the external connections. Tuner 5 is intended for a fine manual tuning of the cavity from outside a vacuum in the range of about  $\pm 80$  kHz.

### MAGNETIC CORRECTOR AND SPECTROMETER

Despite of focusing and steering electric fields, shaping the electron beam at the exit of the RF-deflector, there are extra distortions of electron trajectories up to outlet collimator due to the presence of external fringe magnetic fields. The correcting magnet with the combination of dipole and quadrupole fields (Fig. 4a) is implemented. The dipole field produced with two coils moves the electron beam along Y-axis. The quadrupole field produced with another four coils enables to adjust the tilt of the beam image in YZ-plane (Fig. 4b). The set of electric and magnetic corrections provide an exhaustive fit of the electron beam and the outlet collimator, thus compensating misalignments and an influence of external moderate static magnetic fields.

In case of strong fields from adjoining focusing elements (quads and correctors) or alternating magnetic fields, which cannot be corrected with the technique described above, sectional magnetic shield is foreseen.

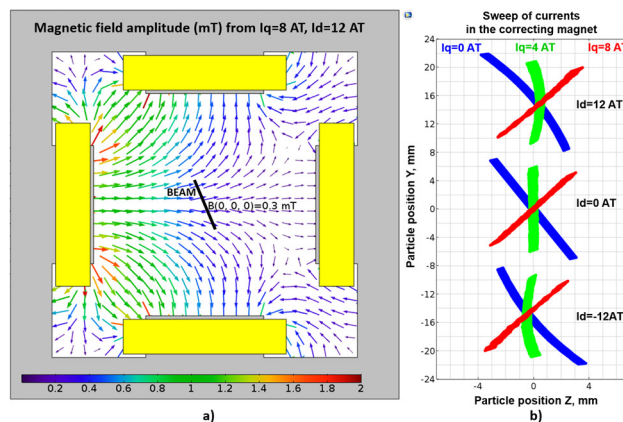


Figure 4: (a) Superposition of dipole and quadrupole fields of the correcting magnet. (b) Cross-sections of the e-beam in the plane of the outlet collimator for different quadrupole  $I_q$  and dipole  $I_d$  coil currents (Ampere·Turns).

The results of measurements can be also influenced by electrons produced due to dissociation of the multicharged ion beam in the target. The signals due to detached electrons are superimposed on the useful signals and distort the measured function. The energy of the detached electrons differs from that of low energy ones, and to decrease an influence of the detached electrons a separation by energy with the help of bending magnet installed downstream of outlet collimator is used. Energy resolution of the 90° magnetic spectrometer is defined mainly by the size of registration collimator. A relatively low value of resolution about 10% is selected to avoid losses of the useful low energy secondary electrons.

### TARGET HEATING LIMITS

The target is a tungsten wire with 0.1 mm diameter, and its maximum heating is limited by rising of an electronic thermionic emission at the temperature about 1700÷1800 K. Experimentally the thermionic emission is manifested as an increase of the background from the beginning to the end of a beam pulse, including the phases outside the bunch. Simulated peak steady temperatures of the target-wire for typical beam parameters are shown in Fig. 5. The mode of 1 Hz is suitable for all beams with pulse duration up to 200  $\mu$ s.

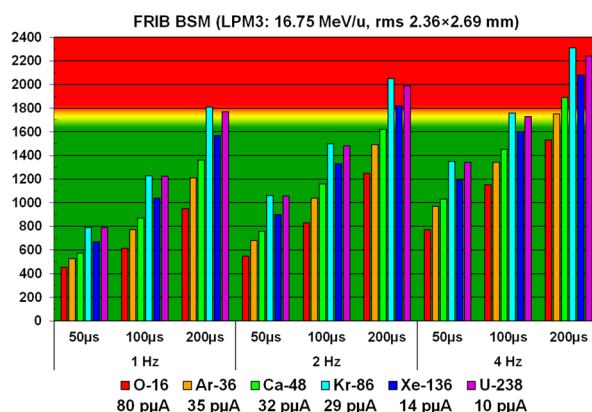


Figure 5: Peak steady temperatures of the target wire for different typical parameters of FRIB ion beams.

Content from this work may be used under the terms of the CC BY 3.0 licence (© 2018). Any distribution of this work must maintain attribution to the author(s), title of the work, publisher, and DOI.



## PHASE RESOLUTION AND ACCURACY

We consider two types of errors: a phase reading error and a phase resolution correspondingly. Due to a phase reading error (accuracy) a measured phase coordinate along the bunch does not correspond to a real one. Due to a finite phase resolution (precision) the measured distributions are smoothed and a fine structure can be lost.

Phase reading errors appear only due to a space charge of the analysed beam, but this effect becomes significant at a pulse electrical current  $>10$  mA.

BSM resolution can be defined as a full width at a half maximum of a spread function for infinitely short bunches. For a real secondary electron beam with a finite width of focusing a phase resolution may be defined as a minimum phase range of secondary electrons, passed through the outlet collimator, thus it can be simulated, considering factors of e-beam optics and dispersion of secondary emission delay, which results in extra defocusing in case of RF-deflecting field turned on. The value of time dispersion is not known exactly, however the experimental estimations give the upper limit of this value  $(4\pm 2)$  ps [3].

Figure 6 shows simulated transverse cross-sections of a e-beam in the plane of the outlet collimator.

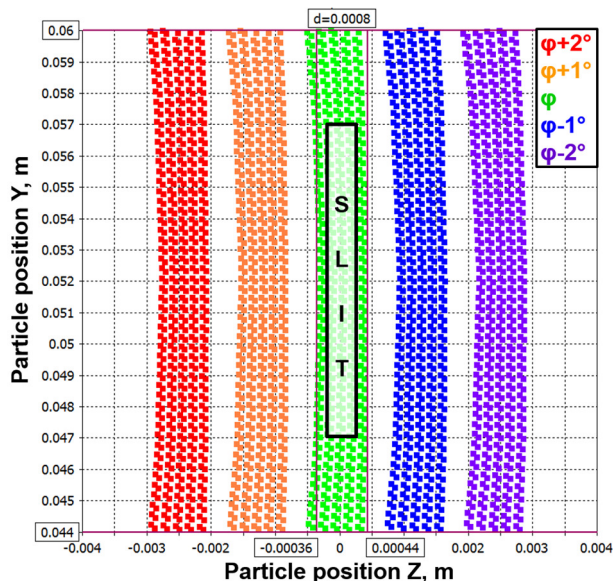


Figure 6: Transverse cross-sections of e-beam in the plane of the outlet collimator at different phases ( $\varphi - 2^\circ \div \varphi + 2^\circ$ ) of the deflecting voltage.

The simulations show, that for the inlet collimator 0.5 mm,  $U_d = 1000$  V the distance between the centers of e-beams frequency sweep in the plane of the outlet collimator  $\Delta Z_0 \approx 1.3$  mm for phases  $\varphi$  and  $\varphi + 1^\circ$ . At the plane of the outlet collimator the beam can be focused down to the size of the inlet collimator slit at  $U_{foc} = 4250$  V, but full width of the beam waist increases up to 0.8 mm due to the RF-defocusing. Thus, a phase resolution  $\Delta\varphi$ :

$$\Delta\varphi = \frac{\text{Width}_{\text{outlet collimator}} + \text{Width}_{\text{e-beam}}}{2 \cdot (Z_0(\varphi) - Z_0(\varphi + 1^\circ))} = 0.5^\circ,$$

at 161 MHz or  $0.25^\circ$  for 80.5 MHz in case of proper e-beam optics for 0.5 mm inlet/outlet collimators.

## LABORATORY TESTS

After complete design, development and fabrication process BSM was assembled (Fig. 7), pumped, tuned and tested for proper operation of all systems: vacuum, RF, high voltage, electronics and control system. Electron beam optics was also tested with the help of thermal electrons: heating the wire target, it is possible to observe through the viewport the thermal electron beam on the phosphor covering the front surface of the outlet collimator plates (Fig. 7 a, b). The e-beam coincides with 0.5 mm slit at  $U_{foc} = 4050$  V and currents in the correcting magnet coils about  $I_q = 2.0$  AT,  $I_d = 12.5$  AT.

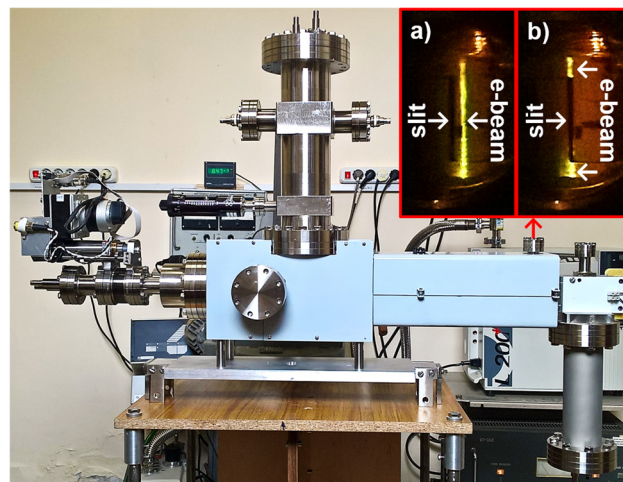


Figure 7: Photo of assembled BSM with magnetic shield. Photos through the viewport: a) Thermal electron beam parallel to the slit of the outlet collimator for comparison. b) Thermal electron beam passing through the 0.5 mm slit of the outlet collimator.

## CONCLUSION

Bunch Shape Monitor was developed for FRIB linac. Special magnetic shield for protection against external fringe magnetic fields and correcting magnet with the combination of dipole and quadrupole fields for compensation of remnant magnetostatic fields and misalignments of BSM elements were implemented. Magnet separation of secondary electrons by energy was foreseen to decrease a possible influence of the electrons detached from the multicharged ions in the wire target. The monitor enables to achieve a quarter of a degree phase resolution for 80.5 MHz RF, that corresponds to about 9 ps, and can be used at any location along the accelerator.

## REFERENCES

- [1] R. Witkover, "A non-destructive bunch length monitor for a proton linear accelerator", *Nucl. Instr. Meth.*, vol. 137, no. 2, pp. 203-211, 1976.
- [2] A. Feschenko, "Technique and instrumentation for bunch shape measurements", in *Proc. RUPAC2012*, Saint-Petersburg, Russia, Oct. 2012, pp. 181-185.
- [3] E. Ernst, H. Von Foerster, "Time dispersion of secondary electron emission", *J. of Appl. Phys.*, vol. 26, no. 6, pp. 781-782, 1955.